Plant Classification from Leaf Textures

Conference Paper · December 2016

DOI: 10.1109/DICTA.2016.7797073

2 authors:

Ana Siravenha
Federal University of Pará

Schubert R. Carvalho
Instituto Tecnológico Vale (ITV)

Plant Classification from Leaf Textures

Ana C. Siravenha
Vale Institute of Technology (ITV)
Belem, PA, Brazil
Email: ana.siravenha@pq.itv.org

Schubert R. Carvalho
Vale Institute of Technology (ITV)
Belem, PA, Brazil
Email: schubert.carvalho@itv.org

***Abstract*—This work describes a methodology for plant classification based on the analysis of leaf textures by combining a multi-resolution technique, such as the two-dimensional (2D) Discrete Wavelet Transform (2D-DWT), statistical models and Gray-Level Co-occurrence Matrices (GLCM) in which some invariance (e.g. rotation and scale) are achieved. As a second step, an Artificial Neural Network (ANN) model is trained for automatic classifying plant species. The proposed approach was tested on the Flavia database. An overall classification accuracy of 91.85% was achieved which demonstrates that plants can be reliably classified using texture samples extracted from leaf tissues.**

I. Introduction

The manual process of plant identification from leaf samples is cumbersome and it is also believed that leaf information alone is insufficient for correct plant classification, because color, venation and shape patterns can present large variability among species [2], [16], [21]. These are some of the reasons why leaf-based plant classification poses challenges for botanists. Nevertheless, plant attributes obtained from its leaves have long been used in botany for identification of plant species, mainly due to the ease of acquiring data samples compared to other plant characters, such as fruits and flowers [12]. Indeed, living tropical plants flower and fruit infrequently.

Over the past two decades, leaf-based algorithms for plant classification have received increased attention [20], [1], [36], [29], [19], [9], [44]. These algorithms mainly focused on leaf venation and shape patterns. Actually, one of the most descriptive attributes of angiosperm leaves is the pattern of venation, which can be defined as the leaf's internal structures that have visually distinct gages and courses. In general, there are up to seven order of venations, and the most important, the higher the vein order the greater the within-species similarities [12]. Vein patterns - if properly decoded - can be explored to build a plant signature and used in plant classification [29], [19]. Due to the visual appearance of leaf surfaces, texture patterns can emerge from venation distributions and from its gray-level intensities [43], [37], [18]. In this work, we use texture analysis techniques for quantifying leaf patterns embedded on venations.

However, there are serious challenges that must be handled to build a robust plant classification methodology. For example, plants have leaves with different sizes producing textures with unequal proportions in width and height leading to external scale variabilities. Moreover, scale variances can also appear internally due to images acquired with different resolutions. Basically, the simplest strategy to obtain scale invariance is to rescale the images to have the same external dimensionality and acquire then with the same resolutions [35], [38], [42], [23], [26]. Furthermore, leaf samples can be acquired at any orientation during the image acquisition stage. In principle, put the leaves always in the same position at the time of the image acquisition, might solve the rotation problem, but lets the system user-dependent, which is undesired in most applications. Therefore, it is necessary to extract rotation invariant attributes [23], [34]. In practical terms, there are two strategies for obtaining rotation invariance for texture analysis [7], [15]: (1) build rotation invariant descriptors, or (2) normalize the texture attributes. The former leads to the construction or adaptation of descriptors that are rotation invariant, without the need of pretreatment texture samples. The latter are based on the normalization of the value of the attributes, without the need of pretreatment both the texture samples and the descriptors. The work described here is based on the second class of techniques.

In this work, we quantify venation patterns from leaf surfaces and use them as statistical attributes to automatically classify plat species. To do so, we combine the power of multi-resolution analysis (MRA) technique, such as the 2D-Discrete Wavelet Transform (DWT), to decompose a natural texture at four levels of resolution and at three orientations ($0°, 45°, 90°$), with the strength of Gray-Level Co-occurrence Matrices (GLCM) at four orientations ($0°, 45°, 90°, 180°$) to analyze the gray-level distribution of leaf venations. In this context, leaves are analyzed as 8-bit gray-level texture images. Scale invariance issues are handled by normalizing the texture attributes, which provided an accurate and simple way to construct a scale invariant feature set. Finally, Artificial Neural Network (ANN) models are employed to classify a plant database called Flavia [41] with thirty two species. The overall classification performance of the proposed method showed that plants can be reliably identified by using patterns extracted from leaf surfaces, such as high and low frequency and gray-level content.

II. Related Work

In order to compare our work with previous ones, we focus on the most relevant works that a similar to our methodology and most important, the ones that used the Flavia dataset. In this study, Wu et al. [41] used four geometric (e.g., leaf

978-1-5090-2896-2/16/$31.00 ©2016 IEEE

Fig. 1. A methodology for quantifying and classifying plant species

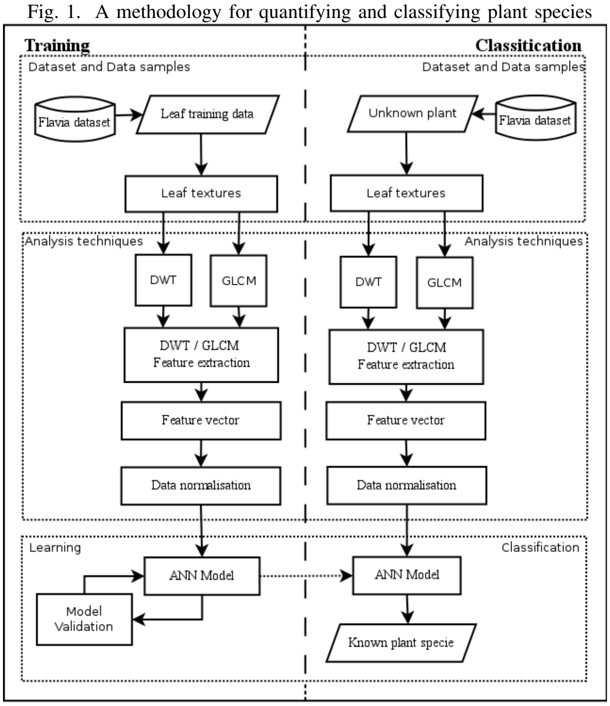

diameter, leaf area, etc.) and twelve morphological features (e.g., perimeter ratio of diameter, vein features, etc.) combined with PCA for training and testing a probabilistic network model for plant classification. The accuracy leaf algorithm was 90% and it was tested with the Flavia dataset. Wu used a morphological descriptor based on shaped area to extract five features from the leaf surface. In a similar way, Gupta [39] also used geometric and morphological features to compare the classification accuracy of three classifiers: SVM-BDT, PNN and Fourier moment. The algorithm was tested with the Flavia dataset. As a result, it was observed that the SVM-BDT provided the best results compared with the other PNN and Fourier Moment, 81.56%, 91.25% and 90.31%, respectively. Both works tested the training classifiers on 320 species, that is 10 for each of the 32 classes. By combining Polar Fourier Transform, geometric, color, texture and vein features to build a feature vector, the method proposed by Kadir [22] achieved a classification accuracy of 94.68%, but it is unclear which validation model was used. The works of Singh [39] and Wu [41] both extracted the same leaf features based on geometric and morphological attributes followed by a dimensionality reduction technique to reduce the feature space and training several classification models. On the other hand Kadir [22] explored different feature patterns, such as Polar Fourier Transform and a combination of 12 geometric and color attributes. However, all three works explored vein features in the same way by using four morphological openings, with disk-shaped structuring element of four different radius measurements, and obtained the ratio between each one and the leaf area.

Differently from these works, the proposed approach in this paper explores leaf surfaces as textures. The analysis step combines 2D-DWT, GLCM and statistical models to build a leaf signature or feature vector with 128 attributes to identify a plant specie into the Flavia dataset. Finally, the feature vectors are subjected to a training phase to build an ANN plant classification model. Table I shows the classification results of the five approaches described in this section.

TABLE I
THIS TABLE SHOWS THE CLASSIFICATION PERFORMANCE OF THE PROPOSED METHOD AGAINST OTHERS THAT USED THE FLAVIA DATASET.

Method	Accuracy (%)
Proposed framework	91.85
SVM-BDT [39]	81.56
PNN [39]	91.25
PNN [41]	90.31
Fourier Moment [39]	90.31
PNN [22]	94.68

III. OUR APPROACH FOR PLANT CLASSIFICATION

Figure 1 shows our approach for plant classification, which combines texture analysis, pattern recognition and machine learning techniques. It is divided mainly in three steps:

- **Dataset and data samples:** We use the Flavia database [41], which is a leaf database with 32 plant species or classes from which a total of 1865 texture samples were extracted for training and classification purposes.
- **Analysis techniques:** To extract a set of features or attributes from leaf textures, we combine a set of analysis techniques such as the 2D-DWT, GLCM and also a data normalization step to avoid possible variations during data transformation.
- **Training & classification:** After data analysis, the normalized feature vectors are subjected to a training or learning phase before classification. Therefore, ANNs are used to measure the discriminative accuracy of these feature vectors. From Figure 1, it is important to mention that learning happens offline and classification is performed online once learning ended.

IV. DATASET AND DATA SAMPLES

This study used experimental data from a public thirty two-classes database provided by Wu et al. [41], which is being considered as a benchmark for comparing the performance of plant classification algorithms and methodologies. Figure 2 depicts a set of leaf samples for each one of the 32 classes (plants are ordered from left to right and top-down, respectively).

The texture samples were acquired to try to capture the maximum order of venations available within each leaf lamina. Differently from Cope et al. [8] –where texture samples capture information from partially secondary to highest venations– our data are acquired from a bigger surface area, covering primary and secondary venations, as well as higher venation patterns, allowing the left and right lamina regions

Fig. 2. This Figure shows leaf samples from the Flavia dataset [41].

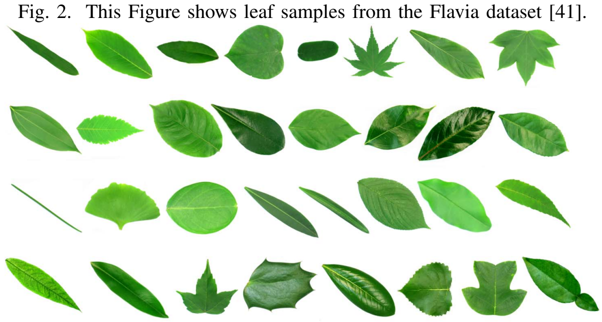

Fig. 3. This Figure shows how data samples are obtained from leaf surfaces. The red box represents the extracted texture region.

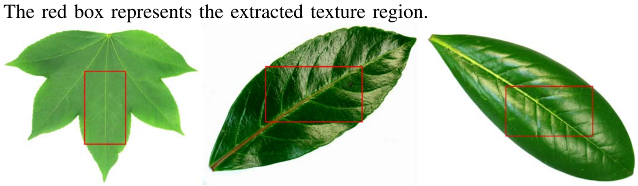

Fig. 4. This figure shows a couple of training textures extracted from the leaf data depicted in Figure 3. Numbers in each sample means the respective plant specie.

(i.e., regions separated by the primary vein) to be analyzed together. In this way, data samples consist of rectangular regions manually extracted from the leaves' surfaces avoiding the leaf base and apex (red boxes in Figure 3), once information from these regions presents more variability according to Ellis et al. [11].

Figure 4 shows one texture sample per specie extracted from the leaf training data. The numbered sequence will be adopted through out the paper to refer to one of the 32 plant species of the Flavia dataset. One can note the similarity in some leaf textures, for example, 3 and 5 and 30 and 31, as well as rotations that are present. The samples were not scale normalized in order to preserve the within-class variance. In fact, Gadermayr et al. [14] observed that, in general, scale invariant features do not outperform the scale variant ones. Thus, following their observation, it will be assumed that the features exhibit a lower within-class variability over multiple scales than the invariant ones. Implicitly, it increases the importance of some scale decompositions (by the DWT) in face of the classification model.

More formally, we represent our data as:

$$\mathrm{F} = [\mathrm{F}^1, \mathrm{F}^2, \dots, \mathrm{F}^\zeta]^\mathrm{T}. \tag{1}$$

Where F is a texture sample, ζ is the number of data samples and T denotes the transpose.

V. Analysis Techniques

According to the texture definition placed previously and as can be observed in Figure 4, there are basically two types of texture patterns that can be explored: 1) the first that comes from the vein structures; and 2) the second that comes from the leaf's surface properties, such as the gray-level intensities. In order to extract texture patterns, we explore the DWT and GLCM techniques. It is important to mention that before feature extraction, textures are gray-level transformed. This transformation stands the importance of gray-scale invariance due to changes in illumination during image acquisition [31].

VI. Discrete Wavelet Transform

At the leave surface the veins that are available for analysis have different sizes or frequencies and orientations, leading to the hard task of defining an optimal resolution and direction for analyzing such structures and extracting texture patterns. To do so, we use a multi-resolution technique, such as the DWT [25], [28], as a first analysis step for building a multi-scale frequency channel decomposition of leaf veins. At this stage, we expect to encapsulate –in the wavelet channels– only the essential patterns of a the vein fabric at different frequencies and orientations. More formally, let F be a leaf texture of $(n \times m)$ size, the DWT of this image can be calculated by using a pyramidal algorithm proposed by Mallat [25]:

$$\mathrm{V}^j = [\phi_x * [\mathrm{F} * \phi_y]_{2n}]_{2m} \tag{2}$$

$$\mathrm{W}_\mathrm{H}^j = [\phi_x * [\mathrm{F} * \psi_y]_{2n}]_{2m} \tag{3}$$

$$\mathrm{W}_\mathrm{V}^j = [\psi_x * [\mathrm{F} * \phi_y]_{2n}]_{2m} \tag{4}$$

$$\mathrm{W}_\mathrm{D}^j = [\psi_x * [\mathrm{F} * \psi_y]_{2n}]_{2m}; \tag{5}$$

where $*$ denotes the convolution operator, (j) is the scale parameter, ϕ is a scale function (i.e. a low pass filter), ψ is a wavelet basis (i.e. a high pass filter) and $(2_n, 2_m)$ are the rows and columns sub-sampling. $\{\mathrm{V}^j\}_{j=1,2,3,\dots,s}$, and $\{\mathrm{W}_\mathrm{H}^j, \mathrm{W}_\mathrm{V}^j, \mathrm{W}_\mathrm{D}^j\}_{j=1,2,3,\dots,s}$ are the wavelet approximation and the coefficients that captures high frequencies in horizontal, vertical and diagonal directions (i.e., $0°, 90°$ and $45°$), respectively.

At the DWT representation, a leaf texture sample (F) is represented by a set of sub-images at different scales (F_w):

$$\mathrm{F}_w = \left[\mathrm{W}_\mathrm{k}^1, \mathrm{W}_\mathrm{k}^2, \dots, \mathrm{W}_\mathrm{k}^s\right] \in \Re^{ks}. \tag{6}$$

Where $\mathrm{k} = \{\mathrm{H}, \mathrm{V}, \mathrm{D}\}$. To give an example, Figure 5 shows a four level decomposition $(s = 4)$ –by using a `Biorthogonal2.2` basis function– of a leaf texture sample extracted from the Aesculus chinensis specie. For better visualization, figure dimensions were kept constant. The impact of the number of wavelet channels on performance of texture classification has been addressed previously by Porter and Lee [34], [24]. The results indicate a non-direct relationship between high level decomposition and high accuracy, indicating that four decompositions is an appropriate choice.

At this fine-to-coarse texture representation, one can observe that at each scale $(j = 1, 2, 3, 4)$ the DWT captures essential structures of the vein fabric. For example, for $j = 1$ high order veins are captured by the wavelet coefficients, but also the primary and secondaries. As j increases (e.g. $j = 4$) most of the information from primary and secondary veins are preserved, but small veins are not captured. At this stage, the major drawback of the DWT is the amount of coefficients it generates, which can lead to the curse of dimensionality phenomena. In order to reduce the feature vector size, we reduce the feature space before training by using a set of statistical measurements and build a wavelet signature –represented by a feature vector– for each plant specie [28], [32], [13], [33], [40].

A wavelet feature vector or signature is built as follows. For each channel $\{\mathrm{W}_{\mathrm{k}}^{j}\}$, we compute a set of nine features as described from equations 7 to 12:

$$e_1^j = \frac{1}{MN}\sum_{u=1}^{M}\sum_{v=1}^{N}|\mathrm{W}_{\mathrm{k}uv}^{j}|^2 \tag{7}$$

$$e_2^j = \frac{1}{MN}\sum_{u=1}^{M}\sum_{v=1}^{N}|\mathrm{W}_{\mathrm{k}uv}^{j}| \tag{8}$$

$$e_3^j = \frac{1}{MN}\sum_{u=1}^{M}\sum_{v=1}^{N}|\mathrm{W}_{\mathrm{k}uv}^{j}|^2 log|\mathrm{W}_{\mathrm{k}uv}^{j}|^2 \tag{9}$$

$$e_4^j = \frac{1}{MN}\sum_{u=1}^{M}\sum_{v=1}^{N}|\mathrm{W}_{\mathrm{k}uv}^{j} - e_2^j| \tag{10}$$

$$\sigma^j = \frac{1}{MN}\sqrt{\sum_{u=1}^{M}\sum_{v=1}^{N}|\mathrm{W}_{\mathrm{k}uv}^{j} - e_2^j|^2} \tag{11}$$

$$F_1^j = \frac{\mu_2^{j1/2}}{m_1^j}, F_2^j = \frac{\mu_3^j}{\mu_2^{j3/2}}, F_3^j = \frac{\mu_4^j}{\mu_2^{j2}}, F_4^j = \frac{\mu_5^j}{\mu_2^{j5/2}}. \tag{12}$$

The normalized moments, F_1^j to F_4^j, were extracted from the central and non-central moments given by equations 13 and 14.

$$\mu_r^j = \frac{1}{MN}\sum_{u=1}^{M}\sum_{v=1}^{N}[\mathrm{W}_{\mathrm{k}uv}^{j} - m_1^j]^r, \tag{13}$$

$$m_1^j = \frac{1}{MN}\sum_{u=1}^{M}\sum_{v=1}^{N}\mathrm{W}_{\mathrm{k}uv}^{j}. \tag{14}$$

A wavelet channel is then represented by:

$$\mathrm{W}_k^j = \left[e_1^j, e_2^j, e_3^j, e_4^j, \sigma^j, F_1^j, F_2^j, F_3^j, F_4^j\right]. \tag{15}$$

As each channel gives nine attributes $(a = 9)$, the new signature $\mathrm{F}_w \in \Re^{aks}$.

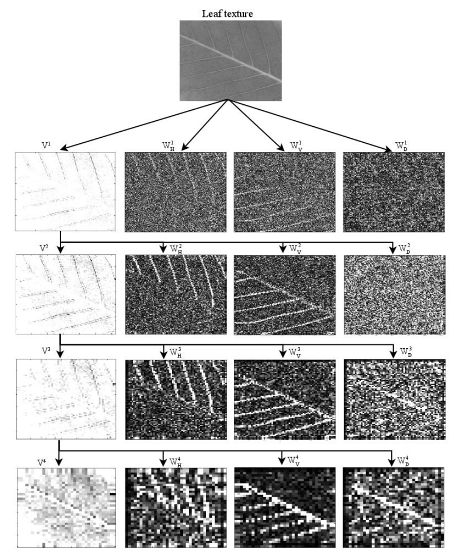

Fig. 5. Pyramid-structured wavelet decomposition of a leaf texture sample from Aesculus chinensis - Chinese horse chestnut

VII. Gray-Level Co-Occurrence Matrices

To still analyze and extract texture patterns, we used gray-level co-occurrence matrices (GLCM), which explores the relative position of the image's neighboring pixels. This technique works by counting the pixel co-occurrences with gray-level values (x, y) at a given distance d [22]. We adjust d to represented texture directions in degrees. As it is hard to know in advance the texture orientation, a set of four standard offsets (α) are used at $0°$, $45°$, $90°$ and $135°$ orientations. These four directions are considered to construct a rotation invariant feature set. Moreover, these four offsets were chosen to follow the directionality of the DWT features. Alike the DWT, GLCM matrices can generate a huge amount of data. To reduce data dimensionality before training, we extract five attributes from each directional GLCM matrix, such as: angular second moment (ASM), inverse different moment (IDM), entropy, contrast and correlation, as shown in Table II.

TABLE II
FEATURE EXTRACTION EQUATIONS FOR A DIRECTIONAL GLCM MATRIX

Feature	Equation
ASM^{α}	$\sum_{l=1}^{L}\sum_{p=1}^{L}(G_{lp}^{\alpha})^2$
IDM^{α}	$\sum_{l=1}^{L}\sum_{p=1}^{L}\frac{G_{lp}^{\alpha}}{1+\lvert l-p\rvert}$
Cr^{α}	$\sum_{l=1}^{L}\sum_{p=1}^{L}\frac{(l-\mu_l^{\alpha})(p-\mu_p^{\alpha})G^{\alpha}(l,p)}{\sigma_l^{\alpha}\sigma_p^{\alpha}}$
E^{α}	$-\sum_{l=1}^{L}\sum_{p=1}^{L}G_{lp}^{\alpha}log(G_{lp}^{\alpha})$
Ct^{α}	$\sum_{l=1}^{L}\sum_{p=1}^{L}\lvert l-p\rvert^2 G_{lp}^{\alpha}$

Where G^{α} is a directional GLCM matrix computed from a texture data sample F_{xy} and $\alpha = \{0°, 45°, 90°, 135°\}$, and

$$\mu_l^{\alpha} = \sum_{l=1}^{L}\sum_{p=1}^{L} l * G_{lp}^{\alpha}, \quad \mu_p^{\alpha} = \sum_{l=1}^{L}\sum_{p=1}^{L} p * G_{lp}^{\alpha}, \tag{16}$$

$$\sigma_l^{\alpha 2} = \sum_{l=1}^{L}\sum_{p=1}^{L} G_{lp}^{\alpha}(l-\mu_l)^2, \quad \sigma_p^{\alpha 2} = \sum_{l=1}^{L}\sum_{p=1}^{L} G_{lp}^{\alpha}(p-\mu_j)^2. \tag{17}$$

A leaf texture sample is then represented by GLCM attributes as (F_g):

$$\mathrm{F}_g = \{\mathrm{ASM}^{\alpha}, \mathrm{IDM}^{\alpha}, \mathrm{Cr}^{\alpha}, \mathrm{E}^{\alpha}, \mathrm{Ct}^{\alpha}\}, \ \mathrm{F}_g \in \Re^{5\alpha}. \tag{18}$$

VIII. Feature Vector

By combining the DWT and GLCM vectors (Equations 6 and 18) $\mathrm{F}_{wg} = [\mathrm{F}_w, \mathrm{F}_g]$. The data matrix F (Equation 1) is then represented as:

$$\mathrm{F} = \left[\mathrm{F}_{wg}^1, \mathrm{F}_{wg}^2 \ \dots \ , \mathrm{F}_{wg}^{\zeta}\right]^{\mathrm{T}} \in \Re^{\zeta \times \eta}. \tag{19}$$

So,

$$\mathrm{F}_{wg}^{\zeta} = [f_{wg}^1, f_{wg}^2, \ \dots f_{wg}^{\eta}] \in \Re^{\eta}, \tag{20}$$

denotes a feature vector representing a plant species - as ($\eta = aks + 5\alpha$) and $s = 4$ - F_{wg} has size $\eta = 128$.

IX. Data normalization

Normalization steps were then applied on DWT and GLCM attributes for reducing data variability during data transformation from sample to sample. In our experiments, normalization techniques, such as log, min-max normalization, and zero-mean normalization (z-score) were tested [17]. Compared with other normalization methods, the min-max normalization data set had the highest accuracy. More formally, let $t_i = f_{wg}^i$ be a feature from a column of the class F_c, the normalized attributes are given by:

$$t_i' = \frac{t_i - min_{\mathrm{F}_c}}{max_{\mathrm{F}_c} - min_{\mathrm{F}_c}}(new_{max_{\mathrm{F}_c}} - new_{min_{\mathrm{F}_c}}) + new_{min_{\mathrm{F}_c}}. \tag{21}$$

$new_{min_{\mathrm{F}_c}} = 0.0$ and $new_{max_{\mathrm{F}_c}} = 1.0$. So, the new attributes $f_{wg}' \in [0.0, 1.0]$. The normalization is done column by column (i.e., per attribute) for each class.

X. Building a Plant Classification Model

After feature extraction, the characteristic vectors are subjected to a training stage. Artificial neural networks (ANN) [5], [10] are some of the most frequently used machine learning techniques in plant classification applications [41], [22], [45]. The backpropagation (BP) learning has become the standard method for ANN training and since it is applicable to several domains it is used to adjust weights and biases in the present work.

The BP training is based on Levenberg-Marquardt (LM) optimization, a derivative of the Newton method [30]. It is a second order learning algorithm that provides fast and efficient training by calculating both gradient and the Jacobian matrix for updating weight and bias values. The algorithm suits the texture patterns as well the ANN topology, consisting of two hidden layers with 26 neurons each with performance index calculated in Mean Squared Error (MSE).

The LM algorithm combines the steepest descent and Gauss-Newton algorithms in a sequence of steps. First, the steepest descent acts around the area with complex curvature until this area is proper to make a quadratic approximation, to then converge the function in a speed up way by the Gauss-Newton algorithm. The classifier was built on the Matlab neural network toolbox [27].

In order to generate an assessment on how well the ANN performs on test data, it was implemented a k-fold cross-validation technique [3]. In this approach the division of data is not a major issue, since every subset is used as training set (k-1 times) and tested once. It has a lower variance than a single hold-out set estimator, which can be very important when the amount of data available is limited, which is not the case here. During the tests, it was used $k = 10$ and the final result is the average accuracy value among all the trials.

XI. Results and Discussion

Plant classification has been performed with biorthogonal and Daubechies wavelet bases. The choice of these filters were preferred due to the trade-off between computational time and filter regularity - the latter is considered an important property for classification of natural textures [32], [13]. A total of 1865 data samples were used in this study and the same training procedure described in Section X was used in all the experiments present in this Section.

A. Evaluating Overall Performance

The first experiment aimed to analyze the influence of leaf scale variances on a set of feature vectors. Fig. 6 presents the classification accuracies for normalized and not normalized textures according to their external scales (i.e., height and width). For both textured data, the Haar (db1) basis achieved the best accuracies in comparison to the feature vectors of the other bases. This performance can be a consequence of its shift invariant property [32]. It means that, the Haar has no overlapping windows, reflecting only changes between adjacent pixel pairs and calculating pairwise averages and differences. The other wavelets —which overlap windows— reflect more changes between pixel intensities, which may represent more redundant information leading to poor classification accuracies.

In general, when the textures were not normalized to handle scale variances, regardless the wavelet basis, classification results were more accurate (63.96%) compared to normalized textures (63.43%). Furthermore normalized data achieved better accuracy results in most of the cases, the classification of normalized textures was at most 5.17% more accurate than the classification of non-normalized data (*Rbior3.3* in Figure 6).

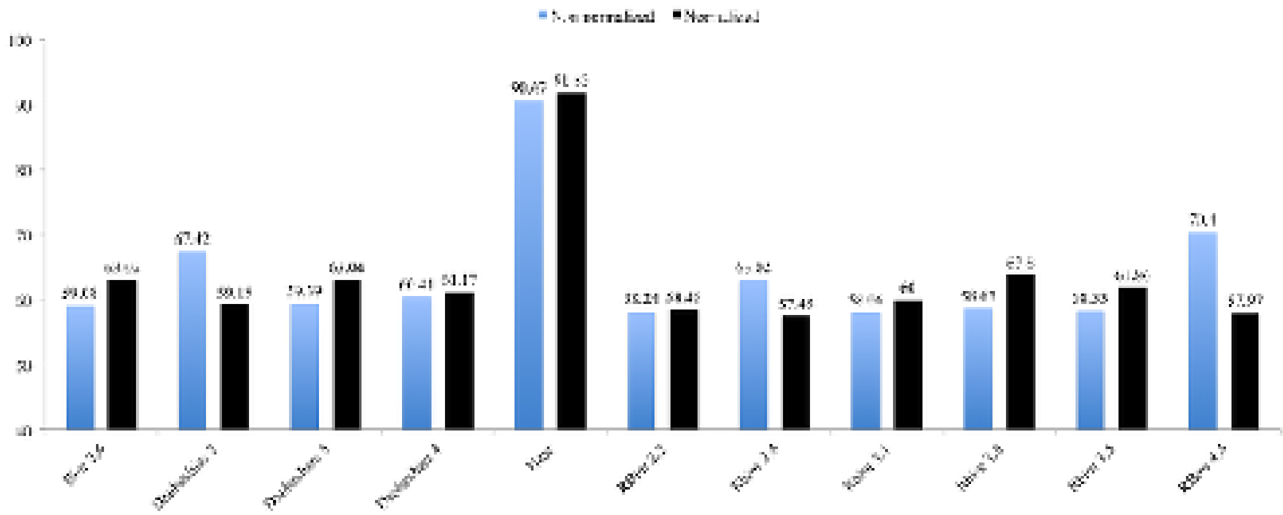

Fig. 6. Results of the proposed feature vector. The black bars shows the model accuracies for the vector non-normalized in scale and the blue bars represent the accuracy values of the normalized textures. Eleven Wavelet bases were experiment by an ANN architecture of two hidden layers with 26 neurons each. The accuracy values represent the average value of k-fold validation.

Moreover, the bases where the high-pass filter is more irregular than the low-pass, presented higher accuracies.

TABLE III
CLASSIFICATION ACCURACIES FOR SELECTED FEATURE VECTORS. FOR WAVELET-BASED ATTRIBUTES THE HAAR BASIS WAS USED.

Feature Vectors	Normalized Textures (%)
Haar Wavelet and GLCM	91.85
Energy	81.81
Entropy	77.91
Energy and Entropy	76.44
Moment F3	68.51
Moment F4	73.48
Moments F3 and F4	66.53
108 Wavelet features	90.45
20 GLCM features	80.00

B. Evaluating Statistical Measurements Performance

In the wavelet texture literature it is common to use a set of statistical measurements, for example, energies, entropies, normalized moments or a combination of them to build a feature vector and test a texture classification methodology [28], [32], [13], [33], [40]. So, the second experiment aimed to analyze the classification accuracy of the DWT and GLCM feature vector, some of the most used statistical measurements alone as well as a combinations of them. Table III shows the classification accuracies for each feature vector analyzed in this experiment. As can be seen, the combined DWT and GLCM feature vector used in this work gave better accuracies compared with the most frequently used feature vectors [28], [32], [13], [33], [40]. Moreover, one can note the discriminative power of the wavelet statistics compared with the GLCM. For example, considering normalized textures, the first line of this table shows the result of the combined DWT and GLCM features (91.85%), the eighth and ninth lines show the accuracy of the 108 wavelet attributes and GLCM isolated (90.45% and 80%, in the same order). So, the GLCM seems to add insignificant improvement on the classification accuracy when combined with the DWT. Other important finding was regarding moments, they gave the lower classification results in comparison with other approaches.

Table IV summarizes some values extracted from the confusion matrix. As can be seen, the sensitivity and specificity are higher than 0.6 in all cases indicating low rate of false responses. In particular, all specificity values are superior to 0.9 and precision also indicates the quality of the results by representing the proportion of the predicted positive cases that were correct. For 26 of 32 classes, this value was superior to 0.9. Finally, classification accuracy was in general higher than 98% for all plant species and the Kappa index is equals to 0.9157. It is important to note that the accuracy results equals or higher than 99.9%, as well as classes with no false positive and/or false negative were excluded by representing the almost unfailing scenario.

XII. CONCLUSION

The manual process of plant identification from leafs is cumbersome. Furthermore, it is also believed that only leaf information is insufficient for correct plant classification. In this paper, we have shown that small leaf image regions carry patterns that can be explored for automatically identifying plant species. By extracting and quantifying these patterns, we built a leaf-based classification framework and validated it with the Flavia dataset. Basically, our framework was divided in three stages. First, data samples extracted from leaf regions were analyzed as textures. Second, a set of feature vectors describing a plant specie was built by combining the 2D DWT and GLCM techniques. As a last stage of the methodology,

TABLE IV
ACCURACY MEASURES OBTAINED FROM THE CONFUSION MATRIX. IT WAS OMITTED CLASSES WITH ACCURACY HIGHER THAN 99.8%, AS WELL AS CLASSES WITH NO FALSE POSITIVE AND/OR FALSE NEGATIVE. THE ACRONYM TP/FP REFERS TO TRUE POSITIVE/FALSE POSITIVE.

Species	TP/FP	Accuracy (%)	Precision	Sensitivity	Specificity	F-Score	G-Score
3	44/06	99.08	0.880	0.80	0.997	0.838	0.839
8	35/02	98.98	0.946	0.67	0.999	0.787	0.798
9	52/04	99.62	0.929	0.95	0.998	0.937	0.937
10	49/21	98.33	0.700	0.83	0.988	0.760	0.762
11	37/02	99.19	0.949	0.74	0.999	0.831	0.838
13	41/01	99.35	0.976	0.79	0.999	0.872	0.877
15	49/16	98.55	0.754	0.82	0.991	0.784	0.785
16	56/18	99.03	0.757	1.00	0.990	0.862	0.870
19	61/04	99.78	0.938	1.00	0.998	0.968	0.969
21	59/03	99.78	0.952	0.98	0.998	0.967	0.967
23	55/10	99.46	0.846	1.00	0.994	0.917	0.920
24	64/07	99.57	0.901	0.98	0.996	0.941	0.942
25	43/17	99.49	0.717	0.80	0.991	0.754	0.755
28	43/09	98.87	0.827	0.78	0.995	0.804	0.804
29	51/05	99.41	0.911	0.89	0.997	0.903	0.903
30	61/03	99.78	0.953	0.98	0.998	0.968	0.968
31	51/07	99.51	0.88	0.96	0.996	0.919	0.920

NN models were constructed from these feature vectors and used for classifying a plant specie of the Flavia database.

We evaluated the performance of eleven wavelet bases and several feature vector combinations. We observed that the DWT contributed more for the increasing in classification accuracy when compared with the GLCM technique. Nonetheless, the combination of both set of attributes (DWT and CLCM) increased a bit the classification accuracy. We believe that the superiority of the DWT descriptors is a consequence of the multi-scale frequency channel decomposition of leaf veins, that encapsulated —in the wavelet channels — essential patterns of a the vein fabric at different frequencies and orientations.

It is common to analyze textures by keeping its size constant (i.e., normalized textures in our examples) [4], [18]. In spite of the data samples used in this work have different sizes due to the way leaf textures were extracted, the classification accuracy increased in the majority of the cases when textured samples were normalized. Another important aspect during the texture classification was the capability of classifying then independent of their rotation angle during image acquisition [6]. By construction, our method handled rotation issues by using the vertical, horizontal and diagonal channels of the DWT and the directional property of the GLCM as shown in Figure 6.

Finally, the NN model required approximately 16 seconds to learn from the data (tested in MATLAB on an iMac 3.5 GHz Intel Core i7 - 32GB 1600MHz DDR3 - running OS X Version 10.8.5). However, once the NN model was built, the time required to make predictions on unseen data was on average $0.6s$, indicating its potential use in real time applications. The performance of our framework showed that plants can be reliably discriminated using patterns extracted from leaf texture images. This is an encouraging avenue for the development of computational tools for plant classification.

REFERENCES

[1] S. Abbasi, F. Mokhtarian, and J. Kittler. Reliable classification of chrysanthemum leaves through curvature scale space. In *Scale-Space*, volume 1252 of *Lecture Notes in Computer Science*, pages 284–295. Springer, 1997.

[2] B. S. Anami, S. S. Nandyal, and A. Govardhan. A combined color, texture and edge features based approach for identification and classification of indian medicinal plants. *International Journal of Computer Applications*, 6(1), 2010.

[3] A.S. Andalib, M.R. Islam, A. Salekin, and M. Abdulla-Al-Shami. Novel approaches for detecting fabric fault using artificial neural network with k-fold validation. In *International Conference on Computer and Information Technology*, pages 55 – 60, 2012.

[4] D. H. Ballard and C. M. Brown. *Computer Vision*. Prentice Hall, New Jersey, USA, 1982.

[5] C. M. Bishop. *Neural Networks for Pattern Recognition*. Oxford University Press, Inc., New York, NY, USA, 1995.

[6] D. Charalampidis and T. Kasparis. Wavelet-based rotational invariant roughness features for texture classification and segmentation. *IEEE Transactions Image Process*, 11:825–837, 2002.

[7] J.-L. Chen and A. Kundu. Rotation and gray scale transform invariant texture identification using Wavelet decomposition and Hidden Markov Model. *IEEE Transactions Pattern Analysis and Machine Intelligence*, 16(2):208–214, 1994.

[8] J. S. Cope, P. Remagnino, S. Barman, and P. Wilkin. Plant texture classification using Gabor co-occurrences. In *ISVC (2)*, volume 6454 of *Lecture Notes in Computer Science*, pages 669–677. Springer, 2010.

[9] F. M. Durgante, N. Higuchi, A. Almeida, and A. Vicentini. Species spectral signature: Discriminating closely related plant species in the amazon with near-infrared leaf-spectroscopy. *Forest Ecology and Management*, 291:240 – 248, 2013.

[10] M. Egmont-Petersen, D. de Ridder, and H. Handels. Image processing with neural networksa review. *Pattern Recognition*, 35(10):2279 – 2301, 2002.

[11] B. Ellis, D. C. Daly, L. J. Hickey, J. V. Mitchell, K. R. Johnson, P Wilf, and S. L. Wing. *Manual of Leaf Architecture*. Comstock Publishing Associates, 2009.

[12] Beth Ellis, Douglas C. Daly, Leo J. Hickey, Kirk R. Johnson, John D. Mitchell, Peter Wilf, and Scott L. Wing. *Manual of Leaf Architecture*. Cornell University Press, 2009.

[13] S. R. Fountain, T. N. Tan, and K. D. Baker. A comparative study of rotation invariant classification and retrieval of texture images. In *Proceedings of British Machine Vision Conference*, pages 266–275, 1998.

[14] M. Gadermayr, S. Hegenbart, and A. Uhl. Scale-adaptive texture classification. In *International Conference on Pattern Recognition*, 2014.

[15] R. C. Gonzalez and R. E. Woods. Digital image processing, 2002.

[16] C-Y Gwo and C-H. Wei. Plant identification through images: Using feature extraction of key points on leaf contours. *Applications in Plant Sciences*, 1(11), 2013.

[17] J. Han, M. Kamber, and J. Pei. *Data mining: concepts and techniques*. Morgan Kaufmann - Elsevier, 2012.

[18] R. M. Haralick and L. G. Shapiro. *Computer and Robot Vision*. Addison-Wesley Longman Publishing Co., Inc., Boston, MA, USA, 1st edition, 1992.

[19] A. N. Hussein and M. I. Saripan S. Mashohor. A texture-based approach for content based image retrieval system for plant leaves images. In *IEEE 7th International Colloquium on Signal Processing and its Applications*, pages 11–14, 2011.

[20] C. Im, H. Nishida, and T. L. Kunii. Recognizing plant species by leaf shapes-a case study of the acer family. In *International Conference on Pattern Recognition - ICPR*, volume 2, pages 1171–1173, 1998.

[21] C. Im, H. Nishida, and T.L. Kunii. Recognizing plant species by leaf shapes-a case study of the acer family. In *International Conference on Pattern Recognition-Volume 2 - Volume 2*, ICPR '98. IEEE Computer Society, 1998.

[22] A. Kadir, L. E. Nugroho, A. Susanto, and P. I. Santosa. Neural network application on foliage plant identification. *International Journal of Computer Applications*, (9):15–22, 2011.

[23] W.-K. Lam and C. K. Li. Classification of rotated and scaled textures by local linear operators. In *Circuits and Systems, 1995. ISCAS'95., 1995 IEEE International Symposium on*, volume 1, pages 243–246. IEEE, 1995.

[24] M.-C. Lee and C.-M. Pun. Classifying rotated textures using Wavelet Packet signatures. In *IEEE International Conference on Acoustics, Speech, and Signal Processing*, pages 2215 – 2218, 2000.

[25] S. Mallat. Multifrequency channel decompositions of images and wavelet models. *IEEE Transactions Acoustics, Speech, and Signal Processing*, 37(12):2091–2110, 1989.

[26] R. Manthalkar, P. K. Biswas, and B. N. Chatterji. Rotation and scale invariant texture features using discrete wavelet packet transform. *Pattern recognition letters*, 24(14):2455–2462, 2003.

[27] MathWorks. Neural network toolbox, 2014.

[28] R.J.E. Merry. *Wavelet Theory and Applications - A literature study*. Eindhoven University of Technology, 2005.

[29] J. Metre, V.and Ghorpade. An overview of the research on texture based plant leaf classification. *CoRR*, abs/1306.4345, 2013.

[30] N. M. Nawi, A. Khan, and M.Z. Rehman. A new Levenberg-Marquardt based back propagation algorithm trained with cuckoo search. *Procedia Technology*, 11:18 – 23, 2013. 4th International Conference on Electrical Engineering and Informatics, {ICEEI} 2013.

[31] T. Ojala, M. Pietika, and T. Maenpaa. Multiresolution gray-scale and rotation invariant texture classification with local binary patterns. *IEEE Transactions on Pattern Analysis and Machine Inteligence*, 24 (7), 2002.

[32] M. Popovic. Texture analysis using 2d wavelet transform: theory and applications. In *proceeding of Telecommunications in Modern Satellite, Cable and Broadcasting Services*, volume 1, pages 148–158, 1999.

[33] C.-M. Pun and M.-C. Lee. Extraction of shift invariant wavelet features for classification of images with different sizes. *IEEE Transactions Pattern Analysis and Machine Intelligence*, 26(9):1228–1233, 2004.

[34] N. Canagarajah R. Porter. Robust rotation-invariant texture classification: Wavelet, Gabor filter and GMRF based schemes. In *IEE Proceedings on Vision, Image and Signal Processing*, pages 180–188, 2000.

[35] H. Romeny and M. Bart. *Geometry-driven diffusion in computer vision*. Kluwer academic Norwell, MA, 1994.

[36] T. Saitoh and T. Kaneko. Automatic recognition of wild flowers. In *International Conference on Pattern Recognition*, pages 507–510, 2000.

[37] N. Sebe and M. S. Lew. *Principles of Visual Information Retrieval*. Advances in Computer Vision and Pattern Recognition - Springer, 2001.

[38] D.-G. Sim, H.-K. Kim, and D.-I. Oh. Translation, scale, and rotation invariant texture descriptor for texture-based image retrieval. In *International Conference on Image Processing*, pages 742–745, 2000.

[39] K. Singh, I. Gupta, and S. Gupta. SVM-BDT PNN and Fourier moment technique for classification of leaf shape. *International Journal of Signal Processing Image Processing and Pattern Recognition*, 3(4):67–78, 2010.

[40] G. Van De Wouwer, P. Scheunders, and D. Van Dyck. Statistical texture characterization from discrete wavelet representations. *IEEE Transactions on Image Processing*, 8:592–598, 1999.

[41] S. G. Wu, F. S. Bao, E. Y. Xu, Y. Wang, Y.-F. Chang, and Q.-L. Xiang. A leaf recognition algorithm for plant classification using probabilistic neural network. In *2007 IEEE International Symposium on Signal Processing and Information Technology*, pages 11–16, 2007.

[42] H. Xiong, T. Zhang, and Y.S. Moon. A translation-and scale-invariant adaptive wavelet transform. *Image Processing, IEEE Transactions on*, 9(12):2100–2108, 2000.

[43] H. Zhang, P. Yanne, and S. Liang. Plant species classification using leaf shape and texture. In *2012 International Conference on Industrial Control and Electronics Engineering (ICICEE)*, pages 2025 – 2028, 2012.

[44] S. Zhang and Y.-K. Lei. Modified locally linear discriminant embedding for plant leaf recognition. *Neurocomputing*, 74:2284 2290, 2011.

[45] Z. Zulkifli, P. Saad, and I.A. Mohtar. Plant leaf identification using moment invariants and general regression neural network. In *2011 11th International Conference on Hybrid Intelligent Systems (HIS)*, pages 430 – 435, 2011.